Distributed localisation of sensors with partially overlapping field-of-views in fusion networks

Conference Paper · July 2016

CITATIONS
0

READS
7

3 authors:

Murat Uney
The University of Edinburgh
25 PUBLICATIONS **95** CITATIONS
SEE PROFILE

Bernard Mulgrew
The University of Edinburgh
337 PUBLICATIONS **4,585** CITATIONS
SEE PROFILE

Daniel Clark
Heriot-Watt University
68 PUBLICATIONS **1,056** CITATIONS
SEE PROFILE

Distributed localisation of sensors with partially overlapping field-of-views in fusion networks

Murat Üney and Bernard Mulgrew
School of Engineering, Institute for Digital Communications,
The University of Edinburgh
EH9 3JL, Edinburgh, UK.
Emails: M.Uney@ed.ac.uk, B.Mulgrew@ed.ac.uk

Daniel Clark
School of Engineering and Physical Sciences,
Heriot-Watt University
EH14 4AS, Edinburgh, UK.
Email: D.E.Clark@hw.ac.uk

***Abstract*—We consider geographically distributed sensor platforms with limited field of views (FoVs) networked together in order to cover a larger surveillance region. Each sensor has a partially overlapping FoV with its neighbours, and, collects both target originated and spurious measurements. We are interested in estimating the locations of the sensors in a network coordinate system using only these measurements. The parameter likelihood of the problem, however, does not scale with the number of sensors as its evaluation requires joint multi-sensor filtering. We propose an approximate likelihood which provides scalability by building upon local single sensor filtering, and, is capable of handling partially overlapping coverage for a pair of sensors. Such scalable approximations for fully overlapping sensor coverages have been recently introduced in a cooperative self-calibration framework in which they are used with pairwise Markov random fields as edge potentials. We use the proposed likelihoods within this framework for distributed self-localisation of sensors in the partially overlapping FoVs case. We provide explicit formulae for the likelihoods and a Monte Carlo algorithm which consists of consecutive likelihood updates and belief propagation steps for estimation –all performed as distributed message passings across the network. We demonstrate the estimation accuracy achieved through simulations with multiple objects and complex measurement models.**

I. Introduction

In a wide area surveillance scenario, we consider networked sensor platforms with moderate resources for sensing, computation, communication and energy. Self-calibration is a highly desired capability for such fusion networks, as imperfect knowledge of these parameters could induce systematic errors and undermine the benefits of networked sensing [1]. It might not be feasible to measure all calibration parameters directly, however. For example, locating sensors in GPS denying environments as in underwater sensing is a challenging task [2], which, in principle, can be done using measurements from non-cooperative objects in the surveillance region.

From this viewpoint, calibration can be treated as parameter estimation in state space models [3] with a particular structure in which likelihoods of the sensor measurements depend on these parameters. In fusion networks, intricate models are used in order to capture a variety of sources of measurement uncertainties including unknown number of manoeuvering targets appearing and disappearing over time, sensor data involving false alarms, missed detections, noise and association uncertainties [4], [5]. Because parameter estimation in this setting involves (multi-object) state estimation via Bayesian recursive filtering, computational complexity becomes an important aspect of any potential solution strategy proposed. In fusion networks, complexity issues are exacerbated by the presence of more than one sensors [6], and scalability with the number of sensors must be addressed, in this context.

One remarkable approach to efficient inference in networks of sensors has been to decompose network wide problems into problems between pairs of sensors using the pairwise Markov random fields (MRFs) framework [7]. These models together with message passing algorithms over them have been used for consistently combining pairwise results in applications including target tracking [8]. In our problem setting, however, these pairwise terms still has combinatorial complexity due to the multi-sensor filtering involved. In order to circumvent this issue, node-wise separable likelihoods have been proposed, which are approximations that build upon local filtering densities [9], [10].

In [9], a separable structure referred to as dual-term node-wise separable likelihoods has been introduced for sensor self-calibration and demonstrated in a self-localisation scenario. The estimation scheme is built upon local RFS filtering and message passing operations for likelihood –or, pairwise edge potential– update, and, belief propagation (BP) iterations (see, e.g., [7]) over the resulting MRF for finding parameter marginals. This algorithm is capable of self-localisation while handling the intracicies of a surveillance scenario as described above. The explicit expressions in [9] for computing these likelihoods are valid, however, for the case when all the sensors collect measurements from the same multi-object scene.

In this work, we consider the case in which sensors have partially overlapping FoVs. We provide explicit formulae for evaluating dual-term separable parameter likelihoods for this case. We then use them with pairwise MRFs and message passing algorithms over them, similar to [9]. The resulting network wide (approximate) model features scalability with the number of sensors as opposed to estimation using exact likelihoods. We use this model for distributed self-localisation of sensors with partially overlapping FoVs.

The structure of the article is as follows: In Section II we give the problem statement. We discuss the combinatorially complex exact solution in Section III. Then, in Section IV,

an overview of the approximation framework is introduced. We present the proposed separable likelihoods in Section V. Details of a Monte Carlo algorithm on this model is given in Section VI, which is demonstrated for sensor self-localisation in Section VII. Finally, we conclude in Section VIII.

II. Problem Statement

Let us consider a graph representation $\mathcal{G} = (\mathcal{V}, \mathcal{E})$ of the network specified by a list of sensor platforms $\mathcal{V} = \{1, ..., N\}$ and bidirectional communication links between pairs of sensors $\mathcal{E} = \{(i,j) | i \text{ and } j \text{ share a communication link}\}$. The neighbours of node i in $\mathcal{G}$ is given by $ne(i) \triangleq \{j | (i,j) \in \mathcal{E}\}$. We assume that $\mathcal{G}$ is connected and might contain cycles.

The objects in the surveillance region $S \subset \mathbb{R}^2$ at time k are represented by a set $X_k \triangleq \{x_k^1, ..., x_k^{M_k}\}$ where M_k is the number of objects at k and each element x_k^m of the set is a state vector $x_k^m \in \mathcal{X}$ of object m. Typically, $x \in \mathcal{X}$ consists of position x^l and velocity x^v fields, i.e., $x = [x^l, x^v]$. In this work, we consider a RFS model [11]: X_k is a realisation of a RFS $\mathbf{X}_k$ which takes values in the space of all finite sets of $\mathcal{X}$ denoted by $\mathcal{F}(\mathcal{X})$. The variable X_{k+1} is given by a Markov shift conditioned on X_k, and, involves a thinning process for disappearing objects (with probability $1 - P_S(x_k^m)$) together with a Markov transition for the objects persisting to appear (with probability $P_S(x_k^m)$) characterised by the conditional density $\pi_k(.|x_k^m)$. A second RFS process known as the birth process with density $b_k(.)$ models newly appearing objects. As a result,

$$X_{k+1} = \tilde{\Pi}_{k+1} \cup B_k, \tag{1}$$

where $B_k \sim b_k(.)$, and, $\tilde{\Pi}_{k+1}$ is the thinned process obtained by selecting elements of $\Pi_{k+1} = \{x_{k+1}^m \sim \pi_k(.|x_k^m)\}_{m=1:M_k}$ with probability $P_s(x_k^m)$.

In our multi-sensor setting, each sensor $j \in \mathcal{V}$ is associated with its own likelihood function which is explicitly conditioned on the sensor location[1]. The likelihood for sensor j is denoted by $l_j(z_{k,j}|x_k; \theta_j)$ where $z_{k,j}$ is the measurement induced by x_k and θ_j is the sensor location.

The FoV of sensor j is denoted by S_j: An object $x \in X_k$ induces a measurent at sensor j with zero probability if $x^l \notin S_j$, and, with probability $P_{D,j}(x^l) > 0$, otherwise. Let us denote the set of object originated measurements by $\tilde{Z}_k^j$. Sensor j also collects spurious measurements C^j due to the surroundings (or, false alarms) which are modelled as a Poisson realisation denoted by $C^j \sim Pois(.; \lambda_{C,j}, s_{C,j}(z))$ where $\lambda_{C,j}$ is the average number of (Poisson distributed) clutter points and $s_{C,j}(z)$ is their spatial density[2]. Therefore, at time k, sensor j receives the set of measurements given by

$$Z_k^j = \tilde{Z}_k^j \cup C_{k,j}.$$

This measurement process leads to a random finite set $\mathbf{Z}_k^j$ which has the conditional density $p_j(Z_k^j|X_k)$ given in terms of the probability of detection profile $P_{D,j}(x)$, false alarm parameters $\lambda_{C,j}$ and $s_{C,j}(z)$, and, uncertainties in object originated measurements $l_j(z^j|x)$ [11, Eq.(12.186)].

Inference in this model when $\theta \triangleq (\theta_1, ..., \theta_N)$ is known involves estimating X_k based on the measurement histories $\{Z_{1:k}^j\}_{j \in \mathcal{V}}$, and is solved by Bayesian recursive filtering [11]. When θ is unknown, its estimation involves finding the so called marginal parameter likelihood of the state space model described above [12], [13]. This likelihood relates the measurement histories $\{Z_{1:k}^j\}_{j \in \mathcal{V}}$ to the network wide unknowns θ – which are sensor locations in this work– and is denoted by $l\left(Z_{1:k}^1, ..., Z_{1:k}^N | \theta\right)$. We consider a random $\boldsymbol{\theta}$ and use this likelihood to update a prior distribution. In other words, we consider the posterior density

$$p(\theta | Z_{1:t}^1, ..., Z_{1:t}^N) \;\propto\; p_0(\theta)\, l\left(Z_{1:t}^1, ..., Z_{1:t}^N | \theta\right), \tag{2}$$

and, would like to find the minimum mean squared error (MMSE) estimate of θ based on this posterior.

In practice, it is reasonable to assume that θ_j takes values from a bounded set $\mathcal{B} \subset \mathbb{R}^2$ (as localisation in a plane is considered) and consequently that θ is bounded. Henceforth, we consider a uniform prior $p_0(\theta)$ over $\mathcal{B}^N$.

III. The exact marginal likelihood of the state space model and a Poisson RFS approximation

The parameter likelihood in (2) decomposes using the chain rule of probabilities [14, Sec.IV] as

$$l\left(Z_{1:t}^1, ..., Z_{1:t}^N | \theta\right) = \prod_{k=1}^{t} p\left(Z_k^1, ..., Z_k^N | Z_{1:k-1}^1, ..., Z_{1:k-1}^N, \theta\right). \tag{3}$$

The multiplicative form admits the interpretation that the factors in the right hand side (RHS) are independent contributions of the sets of measurements collected at k. These contributions relate the current measurement sets to the previous measurement histories through the object state variables. Let us consider explicit expressions for these terms.

For the RFS state space model described in Section II,

$$p\left(Z_k^1, ..., Z_k^N | Z_{1:k-1}^1, ..., Z_{1:k-1}^N, \theta\right) = \int_{\mathcal{X}} \left(\prod_{j \in \mathcal{V}} p_j(Z_k^j | X_k, \theta) \right) p(X_k | Z_{1:k-1}^1, \ldots, Z_{1:k-1}^N, \theta) \delta X_k \tag{4}$$

where the prediction density in (4) is found by Bayesian filtering recursions:

$$p(X_k | Z_{1:k-1}^1, \ldots, Z_{1:k-1}^N, \theta) = \int_{\mathcal{X}} \tilde{\Pi}_k(X_k | X_{k-1}) \times p(X_k | Z_{1:k-1}^1, \ldots, Z_{1:k-1}^N, \theta) \delta X_{k-1}, \tag{5}$$

$$p(X_k | Z_{1:k}^1, \ldots, Z_{1:k}^N, \theta) \propto \left(\prod_{j \in \mathcal{V}} p_j(Z_k^j | X_k, \theta) \right) \times p(X_k | Z_{1:k-1}^1, \ldots, Z_{1:k-1}^N, \theta), \tag{6}$$

and integration over a set variable integrand is defined as [11]

[1]Note that, sensor likelihoods can be selected to depend on any calibration parameter that relates a given object state in a desired reference frame to sensor readings including sensor orientations and other scaling parameters.

[2]Note that, it is possible to use a non-stationary Poisson process model for the clutter. Here, we omit dependency to time for brevity.

$$\int_{\mathcal{S}} f(X)\delta X = \sum_{m=0}^{\infty} \frac{1}{m!} \int_{\mathcal{S}^m} f(\{x_1, \cdots, x_m\}) \mathrm{d}x_1 \cdots \mathrm{d}x_m. \tag{7}$$

Using this likelihood, a joint multi-sensor multi-object tracking problem is solved for given values of θ selected either by an iterative ML approach such as expectation maximisation [15] or a Bayesian MCMC sampling scheme [12]. The computational cost in both cases is dominated by filtering, and, as a result, scalability with the number of sensors needs to be addressed.

Evaluation of (4) in this general form is not tractable unless further simplifications are introduced. One useful simplification that leads to the probability hypothesis density (PHD) filter [16] is obtained by finding the projection of the posterior distributions onto the space of Poisson RFS distributions at every iteration [17], and, propagating this projection instead of the full posterior. Equivalently, the output of the filter is Poisson parameters $(\lambda_k(\theta), s_k(x;\theta))$ which also solve the variational problem

$$\begin{aligned}&(\lambda_k(\theta), s_k(x;\theta)) = \\ &\arg\min_{(\lambda,s)} D(Pois(X_k;\lambda,s,\theta)||p(X_k|Z^1_{1:k},\ldots,Z^N_{1:k},\theta)),\end{aligned} \tag{8}$$

where D above is the Kullback-Liebler divergence [18] between the Poisson model and the updated posterior.

Let us introduce $f_k(X_k;\theta) \triangleq Pois(X_k;\lambda_k(\theta), s_k(x;\theta))$. Substituting f_k in (5) in accordance with the RFS Markov shift in Section II and a Poisson birth process $b_k(.) = Pois(.;\lambda^b_k, s^b_k(x))$ also results with a Poisson predictive density in (4):

$$\begin{aligned}&p(X_k|Z^1_{1:k-1},\ldots,Z^N_{1:k-1},\theta) \\ &\qquad = Pois(X_k;\lambda_{k|k-1}(\theta), s_{k|k-1}(x;\theta))\end{aligned} \tag{9}$$

$$\lambda_{k|k-1}(\theta) = \lambda_{k-1} \int P_s(x) s_{k-1}(x)\mathrm{d}x + \lambda^b_k \tag{10}$$

$$\begin{aligned}s_{k|k-1}(x;\theta) \propto \lambda_{k-1} &\int \pi(x|x')P_s(x')s_{k-1}(x')\mathrm{d}x' \\ &+\lambda^b_k s^b_k(x)\end{aligned} \tag{11}$$

Because of the multi-sensor update (6) involved in (8), however, this strategy (i.e., multi-sensor PHD filtering) also has combinatorial complexity with the number of sensors [19]. The separable likelihoods introduced later in Section IV-B circumvents this problem by building upon single sensor PHD filtering which has favorable complexity properties such as scaling linearly with the number of measurements.

IV. A Dynamic Pairwise MRF Model with Separable Likelihood Edge Potentials

In this section, we outline an approximation to the parameter posterior in (2) further details of which can be found in [9].

A. Pairwise MRFs

Let us make a modelling assumption that $\boldsymbol{\theta}$ with the density given in (2) is Markov with respect to the communication graph $\mathcal{G} = (\mathcal{V}, \mathcal{E})$ introduced in Section II: Node $i \in \mathcal{V}$ is associated with the variable θ_i and the edges of the graph is specified by the availability of communication links. The Markov property is defined as that for sets of nodes A and B, if A and B are separated on $\mathcal{G}$ by another set of nodes C, then, the random variables associated with A, i.e., $\boldsymbol{\theta}_A = \{\boldsymbol{\theta}_i | i \in A\}$, and $\boldsymbol{\theta}_B$ are conditionally independent given $\boldsymbol{\theta}_C$. Let us denote such conditional independence relations by $\boldsymbol{\theta}_A \perp\!\!\!\perp \boldsymbol{\theta}_B | \boldsymbol{\theta}_C$ [20]. All such relations admitted by $\mathcal{G}$ factorise (2) to positive functions (or, potential functions) over the cliques of $\mathcal{G}$ (connected subsets of $\mathcal{V}$) [20]. We select $\mathcal{G}$ to have cliques of only singleton and pairs of nodes, i.e., a pairwise graph. For the case (2) decomposes as

$$\begin{aligned}\tilde{p}(\theta|Z^1_{1:k},...,Z^N_{1:k}) &\propto \prod_{i\in\mathcal{V}} \psi_i(\theta_i) \prod_{(i,j)\in\mathcal{E}} \psi^k_{ij}(\theta_i,\theta_j), \\ \psi_i(\theta_i) &= p_{0,i}(\theta_i), \\ \psi^k_{ij}(\theta_i,\theta_j) &= l(Z^i_{1:k}, Z^j_{1:k}|\theta_i,\theta_j),\end{aligned} \tag{12}$$

where the node potential functions ψ_is are arbitrary priors for θ_i (e.g., uniform distributions over $\mathcal{B}$) and the edge potentials ψ^k_{ij}s are predictive parameter likelihoods for the pairs (i,j)s based on sensor histories up to time k. These edge potentials have the time-recursive structure in (3), i.e.,

$$\begin{aligned}\psi^k_{ij}(\theta_i,\theta_j) &= \prod_{t=0}^{k-1} p(Z^i_{t+1}, Z^j_{t+1}|Z^i_{1:t}, Z^j_{1:t}, \theta_i, \theta_j) \\ &= \psi^{k-1}_{ij}(\theta_i,\theta_j) p(Z^i_k, Z^j_k|Z^i_{1:k-1}, Z^j_{1:k-1}, \theta_i, \theta_j),\end{aligned} \tag{13}$$

and render a dynamical MRF.

MMSE estimation on the MRF model in (12) can be carried out as an iterative message passing algorithm, i.e., nodes of $\mathcal{G}$ send messages to their neighbours and combine the incoming messages with the local information in consecutive steps. The MMSE estimate of θ is a concatenation of the MMSE estimates of θ_is with their marginal distributions. The marginal densities of (12) can be computed using Belief Propagation (BP) [21] in which nodes maintain distributions over their local variables (or, "belief"s) and update them based on messages from their neighbours using

$$m_{ji}(\theta_i) = \int \psi^k_{ij}(\theta_i,\theta_j)\psi_j(\theta_j) \prod_{i'\in ne(j)\setminus i} m_{i'j}(\theta_j)\,\mathrm{d}\theta_j, \tag{14}$$

$$\tilde{p}_i(\theta_i) = k_i \psi_i(\theta_i) \prod_{j\in ne(i)} m_{ji}(\theta_i), \tag{15}$$

for all $i \in \mathcal{V}$, where k_is are scale factors.

Over a cycle-free $\mathcal{G}$, BP node beliefs (i.e., $\tilde{p}_i$s) in (15) converges to the marginals of (12) in a finite number of steps [21]. When $\mathcal{G}$ contains cycles, BP message and update equations are still well defined. The fixed points of the loopy algorithm exist provided that some conditions are satisfied (see, for example [20] and the references therein) and are approximations of the marginals seeked. Loopy BP has been very successful in distributed estimation in sensor network applications [7], [8]. We provide similar benefits in our problem setting by using the MRF model introduced above.

B. Dual term node-wise separable edge potentials

The MRF model in (12) and (13) decompose the global parameter estimation task into subtasks involving pairs of sensors. The pairwise likelihood in (13), however, still suffers from the combinatorial complexity steming from multi-sensor filtering discussed in Section III – when (3)–(6) is considered for a pair of sensors. We give a brief outline of separable likelihoods [9] which circumvent this issue by building upon terms output by local filtering with RFS densities.

Let us consider approximating the edge potentials (13) with a product of the form

$$\tilde{\psi}^k_{ij}(\theta_i,\theta_j) = l^k_{ij}(\theta_i,\theta_j) l^k_{ji}(\theta_i,\theta_j) \tag{16}$$

where l^k_{ij} and l^k_{ji} can be computed using separate single sensor filters with the histories $Z^j_{1:k}$ and $Z^i_{1:k}$, respectively – as opposed to joint filtering of these histories necessary to compute (13). We do so by replacing the update term in (13) with

$$q(Z^i_k, Z^j_k | Z^i_{1:k-1}, Z^j_{1:k-1}, \theta_{i,j}) \approx p(Z^i_k, Z^j_k | Z^i_{1:k-1}, Z^j_{1:k-1}, \theta_{i,j}), \tag{17}$$

$$q(Z^i_k, Z^j_k | Z^i_{1:k-1}, Z^j_{1:k-1}, \theta_{i,j}) \triangleq p(Z^i_k | Z^j_{1:k-1}, \theta_{i,j}) p(Z^j_k | Z^i_{1:k-1}, \theta_{i,j}), \tag{18}$$

which is also a conditional probability density over (Z^i_k, Z^j_k).

This approximation is useful in our problem setting in that its factors depend on single sensor histories and hence can be evaluated using local filtering, only. Moreover, the computations involved can be performed in a message passing fashion [9]. The approximation quality in terms of the Kullback-Leibler (KL) divergence [18] between the centralised update term on the RHS of (17) with respect to its approximation in the left hand side (LHS) is upper bounded by the difference between the total local state prediction entropies and the entropies of the joint prediction and its most uncertain single sensor update [9, Corollary4.2], i.e.,

$$\begin{aligned} D(p||q) \leq\ & H(\boldsymbol{X}_k | \boldsymbol{Z}^i_{1:k-1}, \boldsymbol{\theta}_{i,j}) + H(\boldsymbol{X}_k | \boldsymbol{Z}^j_{1:k-1}, \boldsymbol{\theta}_{i,j}) \\ & - H(\boldsymbol{X}_k | \boldsymbol{Z}^i_{1:k-1}, \boldsymbol{Z}^j_{1:k-1}, \boldsymbol{\theta}_{i,j}) \\ & - \max\{ H(\boldsymbol{X}_k | \boldsymbol{Z}^i_k, \boldsymbol{Z}^i_{1:k-1}, \boldsymbol{Z}^j_{1:k-1}, \boldsymbol{\theta}_{i,j}), \\ & \qquad H(\boldsymbol{X}_k | \boldsymbol{Z}^j_k, \boldsymbol{Z}^i_{1:k-1}, \boldsymbol{Z}^j_{1:k-1}, \boldsymbol{\theta}_{i,j}) \}. \end{aligned} \tag{19}$$

where H denotes the Shannon Entropy [18].

Note that the first two terms in the RHS of (19) measure the uncertainty in the object state predictions made locally. It can also be shown that these terms are independent from the distribution of $\boldsymbol{\theta}_{i,j}$ (i.e., sensor location distributions). Overall, this bound measures the amount of uncertainty reduced when state predictions and estimations are based on joint sensor histories instead of single sensor histories. A smaller difference suggests a better quality of approximation which should be expected as the local prediction densities become more concentrated around a single point in the state space.

A typical example in which tracking filters provide a fair accuracy in predicting and estimating object locations is range-bearing sensing. An alternative example in which these conditions cannot be guaranteed to be satisfied is bearing-only sensing: The local filtering distributions typically have probability masses spread around the line-of-sights whereas use of joint sensor histories would lead to accurate state prediction and estimation. This yields relatively high values on the RHS of (19) and centralised schemes should be preferred for this modality [22].

The use of the node-wise separable term in (18) to update the dynamic MRF edge potentials given by (13) leads to the following recursive formulae:

$$\begin{aligned} \tilde{\psi}^k_{ij}(\theta_i,\theta_j) &= \tilde{\psi}^{k-1}_{ij}(\theta_i,\theta_j) q(Z^i_k, Z^j_k | Z^i_{1:k-1}, Z^j_{1:k-1}, \theta_{i,j}), \\ &= \prod_{t=0}^{k-1} p(Z^i_t | Z^j_{1:t-1}, \theta_{i,j}) p(Z^j_t | Z^i_{1:t-1}, \theta_{i,j}), \\ &= l^k_{ij}(\theta_i,\theta_j) l^k_{ji}(\theta_i,\theta_j), \end{aligned} \tag{20}$$

where the node-wise terms in (16) are the products of individual node-wise separable update factors over time defined in a recursive fashion:

$$l^k_{ij}(\theta_i,\theta_j) \triangleq l^{k-1}_{ij}(\theta_i,\theta_j) p(Z^i_k | Z^j_{1:k-1}, \theta_{i,j}), \tag{21}$$

$$l^k_{ji}(\theta_i,\theta_j) \triangleq l^{k-1}_{ji}(\theta_i,\theta_j) p(Z^j_k | Z^i_{1:k-1}, \theta_{i,j}). \tag{22}$$

Let us consider explicit expressions for the update term above when the RFS state space model described in Section II is used. We first introduce some notation: Let us denote by $[X_k]_j$ the set X_k with its elements shifted to a coordinate frame centered at sensor j. Because the measurements of sensor j is collected in this frame, the argument of the posterior density obtained from local filtering, i.e., $p_j(X_k|Z_{1:k})$, is actually in this coordinate system, which can explicitly be shown as $p_j([X_k]_j|Z^j_{1:k})$.

The transformation from a sensor j centric description of the surveillance region to a sensor i centric frame is found as

$$[X_k]_i = [X_k]_j + \theta_j - \theta_i$$

were the notation on the RHS is a shorthand for $\{ x \,|\, x_j \in [X_k]_j \wedge x = x_j + \theta_j - \theta_i \}$. Let us denote this transformation (from sensor j's frame to that of i) by

$$\tau(X; \theta_{j,i}) \triangleq X + \theta_j - \theta_i. \tag{23}$$

Using this notation, and the the conditional independence of sensor measurements (Sec. II), i.e., $\mathbf{Z}^i_k \perp\!\!\!\perp \mathbf{Z}^j_{1:k-1} | \mathbf{X}_k, \boldsymbol{\theta}_{i,j}$, the update term in (21) can easily be found as

$$p(Z^i_k | Z^j_{1:k-1}, \theta_{i,j}) = \int p\left(Z^i_k | \tau([X_k]_j, \theta_{j,i})\right) p_j([X_k]_j | Z^j_{1:k-1}) \delta[X_k]_j, \tag{24}$$

where the set integral above is defined in (7).

Note that (24) is valid for arbitrary sensor FoVs as the RFS likelihood captures S_is through the detection profiles $P_{D,i}(x)$s (Sec. II). When finding closed form expressions for

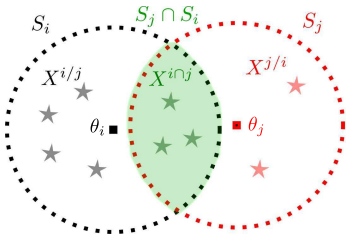

Fig. 1. Two sensors located at θ_i and θ_j with partially overlapping field of views (FoVs): Sensor i (black square) and j (red square) collect measurements from the objects inside their FoVs shown by S_i and S_j, respectively.

the set integral in (24), however, attention should be paid to the underlying assumptions. For example, when p_j is a Poisson density $Pois(.;\lambda_{k|k-1,j}, s_{k|k-1,j})$ computed possibly using the PHD filter [16], a simple form is found [9]:

$$p(Z_k^i|Z_{1:k-1}^j,\theta_{i,j}) = \exp\left(-\lambda_{C,i}-\lambda_{k|k-1,j}(\theta_{i,j})\int P_{D,i}(x)\, s_{k|k-1,j}(x;\theta_{i,j})\mathrm{d}x\right)\times \prod_{z\in Z_k^i}\left(\lambda_{C,i}s_{C,i}(z)+\lambda_{k|k-1,j}(\theta_{i,j})\times \int P_{D,i}(x)\, l_i(z|x)\, s_{k|k-1,j}(x;\theta_{i,j})\mathrm{d}x\right), \quad (25)$$

where subscript i signifies that the quantity belongs to the measurement model of node i and the dependence of the quantities on $\theta_{i,j}$ is shown explicitly. This equation is valid, however, when there are no objects observed by sensor i but not by sensor j, i.e., the case of fully overlapping sensor coverages. Next, we present explicit expressions for evaluating (24) in the case of partially-overlapping FoVs S_i and S_j.

V. Dual-term likelihoods for sensors with partially overlapping FoVs

Let us consider Figure 1 and let X_k represent the set of targets observed by either sensors i or j, modelled with a Poisson point process $\boldsymbol{X}_k$ over $S_i \cup S_j$[3]. We will need to define target processes in the partitions of the sensor FoVs $S_{i/j} \triangleq S_i/S_j$, $S_{j/i} \triangleq S_j/S_i$ and $S_{i\cap j} \triangleq S_i \cap S_j$ in Figure 1, which depend on θ_i and θ_j. In particular, let us define, $X_k^{i/j}$, $X_k^{j/i}$, and $X_k^{i\cap j}$ respectively, i.e.,

$$X_k^{i/j} \triangleq X_k \cap S_{i/j},\quad X_k^{j/i} \triangleq X_k \cap S_{j/i},\quad X_k^{j\cap i} \triangleq X_k \cap S_{j\cap i},$$

Doing so corresponds to marking the elements of X_k, because $S_{i/j}$, $S_{j/i}$ and $S_{i\cap j}$ are disjoint sets. Therefore, we decompose $\boldsymbol{X}_k$ as a superposition of independent Poisson processes (see, for example, [23, Chp.5]). Because sensor j can estimate only X_k^j, X_k in (24) should be replaced with X_k^j:

$$p(Z_k^i|Z_{1:k-1}^j,\theta_{i,j}) = \int p(Z_k^i|\tau([X_k^j]_j,\theta_{j,i}))p_j([X_k^j]_j|Z_{1:k-1}^j)\delta[X_k^j]_j. \quad (26)$$

[3]To be precise, X_k has a velocity component, so, $\boldsymbol{X}_k$ is a Poisson process over $(S_i \cup S_j)\times\mathbb{R}^2$. We omit the Cartesian products in all definitions here, for brevity.

Moreover, $X_k^j = X_k^{j/i} \cup X_k^{i\cap j}$ and using the independence of these processes, we find

$$p_j(X_k^j|Z_{1:k-1}^j) = p_{j\cap i}(X_k^{j\cap i}|Z_{1:k-1}^j;\theta_{i,j}) \times p_{j/i}(X_k^{j/i}|Z_{1:k-1}^j;\theta_{i,j}). \quad (27)$$

where the conditioning on $\theta_{i,j}$ is to highlight that $X_k^{j\cap i}$ and $X_k^{j/i}$ are defined given $\theta_{i,j}$.

Because sensor i cannot observe $X_k^{j/i}$ (i.e., $P_{D,i}(x) = 0$ outside the FoV of sensor i in (24)), this term has no bearing on the likelihood $p(Z_k^i|[X_k^j]_i)$. Therefore, $p(Z_k^i|[X_k^j]_i) = p(Z_k^i|[X_k^{j\cap i}]_i)$ and substituting (27) in (26) leads to

$$p(Z_k^i|Z_{1:k-1}^j,\theta_{i,j}) = \int p(Z_k^i|[X_k^{j\cap i}]_i) \times p_{j\cap i}\left(\tau^{-1}([X_k^{j\cap i}]_i,\theta_{j,i})|Z_{1:k-1}^j\right)\delta[X_k^{j\cap i}]_i. \quad (28)$$

Moreover, given $p_j(.|Z_{1:k-1}^j) = Pois(.;\lambda_{k|k-1,j}, s_{k|k-1,j})$, the predictive density inside the set integral above can easily be found using the independence relation in (27) as follows:

$$\begin{aligned} p_{j\cap i}(X_k^{j\cap i}|Z_{1:k-1}^j) &= e^{-\lambda_{k|k-1,j\cap i}}\prod_{x'\in X_k^{j\cap i}} s_{k|k-1,j\cap i}(x) \\ \lambda_{k|k-1,j\cap i} &= \lambda_{k|k-1,j}\int \mathbb{I}_{S_{j\cap i}}(x)s_{k|k-1,j}(x')\mathrm{d}x' \\ s_{k|k-1,j\cap i}(x) &= \frac{\mathbb{I}_{S_{j\cap i}}(x)s_{k|k-1,j}(x)}{\int \mathbb{I}_{S_{j\cap i}}(x')s_{k|k-1,j}(x')\mathrm{d}x'} \end{aligned} \quad (29)$$

where $\mathbb{I}_{S_{j\cap i}}$ is the indicator function for the set $S_{j\cap i}$.

Second, we decompose the observation process at sensor i into independent components. Note that Z_k^i is already a superposition of the measurements induced by X_k^i and an independent clutter processes, denoted by $\tilde{Z}_k^i$ and $C_{k,i}$ in Section II. As per the likelihood term inside the integral in (28), we note that $X_k^i = X_k^{j\cap i}\cup X_k^{i/j}$, and, further mark the components of $\tilde{Z}_k^i$ as those originated from $X_k^{i\cap j}$ and those from $X_k^{i/j}$, i.e.,

$$Z_k^i = \tilde{Z}_k^{i\cap j} \cup \tilde{Z}_k^{i/j} \cup C_{k,i}. \quad (30)$$

Let us redefine the "spurious" measurements contained in Z_k^i as $\tilde{C}_{k,i} \triangleq \tilde{Z}_k^{i/j} \cup C_{k,i}$. The distribution from which $\tilde{Z}_k^{i/j}$ is generated from can be shown to have the density

$$p(\tilde{Z}_k^{i/j}) = \int p(\tilde{Z}_k^{i/j}|X_k^{i/j})p_{i/j}(X_k^{i/j}|Z_{1:k}^i)\delta X_k^{i/j}. \quad (31)$$

The posterior density inside the set integral above is a Poisson and given the local posterior of sensor i, i.e., $Pois(.;\lambda_k^i, s_k^i)$, can be found as follows:

$$\begin{aligned} p_{i/j}(X_k^{i/j}|Z_{1:k}^i) &= Pois(X_k^{i/j};\lambda_k^{i/j}, s_k^{i/j}) \\ \lambda_k^{i/j} &= \lambda_k^i\int_{S_{i/j}} s_k^i(x)\mathrm{d}x \\ s_k^{i/j}(x) &= \frac{\mathbb{I}_{S_{i/j}}(x)s_{k,i}(x)}{\int \mathbb{I}_{S_{i/j}}(x')s_{k,i}(x')\mathrm{d}x'} \end{aligned} \quad (32)$$

Using the expression above and the measurement model in

Section II, (31) can be found as a Poisson with the following parameters

$$p(\tilde{Z}_k^{i/j}) = Pois(.; \lambda_{Z,k}^{i/j}, s_{Z,k}^{i/j}),$$
$$\lambda_{Z,k}^{i/j} = \lambda_k^{i/j} \int P_{D,i}(x) s_k^{i/j}(x) \mathrm{d}x,$$
$$s_{Z,k}^{i/j}(z) = \frac{\lambda_k^{i/j}}{\lambda_{Z,k}^{i/j}} \int l_i(z|x) P_{D,i}(x) s_k^{i/j}(x) \mathrm{d}x. \quad (33)$$

As a result, the evaluation of (28) above has the same Poisson form as in (25), with the difference that the quantities related to the spurious measurements are replaced with those modelling the superposition of $\tilde{Z}_k^{i/j}$ and C_i, as opposed to only C_i, and the quantities pertaining $X_{k|k-1}$ replaced with ones modelling $X_{k|k-1}^{i\cap j}$:

$$p(Z_k^i | Z_{1:k-1}^j, \theta_{i,j}) =$$
$$\exp\Bigg(- \lambda_{Z,k}^{i/j} - \lambda_{C,i} - \lambda_{k|k-1,j\cap i}(\theta_{i,j}) \times \int P_{D,i}(x)\, s_{k|k-1,j\cap i}(x;\theta_{i,j}) \mathrm{d}x \Bigg)$$
$$\times \prod_{z\in Z_k^i} \Bigg(\lambda_{Z,k}^{i/j} s_{Z,k}^{i/j}(z) + \lambda_{C,i} s_{C,i}(z) + \lambda_{k|k-1,j\cap i}(\theta_{i,j}) \times \int P_{D,i}(x)\, l_i(z|x)\, s_{k|k-1,j\cap i}(x;\theta_{i,j}) \mathrm{d}x \Bigg). \quad (34)$$

The expression above can be estimated using Monte Carlo methods with a negligible amount of computations added to that for estimating (25) which is linear in the number of measurements. The extra computations mainly involves labelling of the particles as being in $S_{i/j}$, $S_{i\cap j}$, or $S_{j/i}$ and finding weighted sums over those labels. This topic is discussed in detail, in the next section.

VI. A Monte Carlo self-localisation algorithm for sensors with partially overlapping FoVs

In this section, we introduce a multi-sensor localisation multi-target tracking algorithm using particle representations and Monte Carlo computations [24]. For local filtering, we use a Sequential MC realisation of the PHD filter [25] using which node j finds a Poisson model for X_{k-1}^j denoted by $Pois(.; \hat{\lambda}_{k-1,j}, \hat{S}_{k-1,j}(dx))$. Here, $\hat{S}_{k-1,j}(dx)$ is an empirical distribution encoded by the set of particles $\{x_{k-1,j}^{(m)}, \zeta_{k-1,j}^{(m)}\}_{m=1}^M$, i.e.,

$$\hat{S}_{k-1,j}(dx) = \sum_{m=1}^{M} \zeta_{k-1,j}^{(m)} \delta_{x_{k-1,j}^{(m)}}(dx), \quad (35)$$

where δ_x is the Dirac measure concentrated at x.

The predictive Poisson model in (27) with its argument in the coordinate frame of sensor i is found as in the prediction stage of the SMC PHD filter [25]:

$$\hat{\lambda}_{k|k-1,j}(\theta_{i,j}) = \lambda_{k-1,j} \sum_m \zeta_{k-1,j}^{(m)} P_S(x_{k-1,j}^{(m)} + \theta_j - \theta_i),$$
$$\hat{S}_{k|k-1,j}(dx;\theta_{i,j}) = \sum \zeta_{k|k-1,j}^{(m)} \delta_{x_{k|k-1,j}^{(m)}}(dx), \quad (36)$$
$$x_{k|k-1,j}^{(m)} \sim \pi(x | x_{k-1,j}^{(m)} + \theta_j - \theta_i),$$
$$\zeta_{k|k-1,j}^{(m)} = \frac{\zeta_{k-1,j}^{(m)} P_S(x_{k-1,j}^{(m)} + \theta_j - \theta_i)}{\sum_{m'} \zeta_{k-1,j}^{(m')} P_S(x_{k-1,j}^{(m')} + \theta_j - \theta_i)}.$$

The predictive density in (28) for $X_k^{j\cap i}$ is then found using (36) in (29):

$$\hat{\lambda}_{k|k-1,j\cap i} = \hat{\lambda}_{k|k-1,j} \sum_m \zeta_{k|k-1,j}^{(m)} \mathbb{I}_{S_{j\cap i}}(x_{k|k-1,j}^{(m)})$$
$$\hat{S}_{k|k-1,j\cap i}(dx) = \frac{\sum_{m'|x_{k|k-1,j}^{(m')} \in S_{j\cap i}} \zeta_{k|k-1,j}^{(m')} \delta_{x_{k|k-1,j}^{(m')}}(dx)}{\sum_m \zeta_{k|k-1,j}^{(m)} \mathbb{I}_{S_{j\cap i}}(x_{k|k-1,j}^{(m)})}$$

The PHD filter local to node i provides a Poisson model for X_k^i simultaneously, consisting of $\hat{\lambda}_{k,i}$ and a set of particles $\{x_{k,i}^{(m)}, \zeta_{k,i}^{(m)}\}_{m=1}^M$. Using these quantities, the parameters of the measurement process $\tilde{Z}_k^{i/j}$ in (31),(given by (32)–(33)) are found as follows:

$$\hat{\lambda}_k^{i/j} = \hat{\lambda}_k^i \sum_m \zeta_{k,i}^{(m)} \mathbb{I}_{S_{i/j}}(x_{k,i}^{(m)})$$
$$\hat{S}_{k|k}^{i/j}(dx) = \frac{\sum_{m'|x_{k,i}^{(m')} \in S_{i/j}} \zeta_{k,i}^{(m')} \delta_{x_{k,i}^{(m')}}(dx)}{\sum_m \zeta_{k,i}^{(m)} \mathbb{I}_{S_{i/j}}(x_{k,i}^{(m)})}$$
$$\hat{\lambda}_{Z,k}^{i/j} = \hat{\lambda}_{k|k}^{i/j} \sum_{m'|x_{k,i}^{(m')} \in S_{i/j}} \zeta_{k,i}^{(m')} P_{D,i}(x_{k,i}^{(m')})$$
$$\hat{s}_{Z,k}^{i/j}(z) = \frac{\hat{\lambda}_{k|k}^{i/j}}{\hat{\lambda}_{Z,k}^{i/j}} \sum_{m'|x_{k,i}^{(m')} \in S_{i/j}} P_{D,i}(x_{k,i}^{(m')}) \zeta_{k,i}^{(m')} l_i(z|x_{k,i}^{(m')}) \quad (37)$$

Finally, the update term in (34) can be found by substituting from the Monte Carlo estimates we have found so far to (34). Let us denote this estimate by $\hat{p}(Z_k^i | Z_{1:k-1}^j, \theta_{i,j})$.

We compute these estimates for L many $\theta_{i,j}^{(l)}$ points generated from $p_i(\theta_i)$ and $p_j(\theta_j)$. Therefore, at each time step k, the update term $\hat{p}(Z_k^i | Z_{1:k-1}^j, \theta_{i,j}^{(l)})$ is computed for all $\{\theta_{i,j}^{(l)}\}_{l=1}^L$ and for all $j \in ne(i)$ in order to update $\{\hat{l}_{i,j}^k(\theta_i^{(l)}, \theta_j^{(l)})\}_{l=1}^L$. At the last step of the time window $k = t$, the estimated node wise terms are exchanged and the edge potentials $\{\hat{\psi}_{i,j}^k(\theta_i^{(l)}, \theta_j^{(l)})\}_{l=1}^L$ are found by simply taking the element-wise product of the node-wise separable terms (Eq.(16)).

Now, let us adopt the sampling approach detailed in [9, Sec.VI] for carrying out LBP belief update and messaging in (15) and (14), respectively. Given L equally weighted samples from $\tilde{p}_i(\theta_i)$, i.e.,

$$\theta_i^{(l)} \sim \tilde{p}_i(\theta_i), \text{ for } l = 1, \ldots, L, \quad (38)$$

the edge potetials are evaluated as discussed above to obtain

$$\psi_{ij}^t(\theta_i^{(l)}, \theta_j^{(l)}) \text{ for } l = 1, \ldots, L. \quad (39)$$

Consider the BP message from node j to i in (14). Suppose that independent identically distributed (i.i.d.) samples from the (scaled) product of the jth local belief and the incoming messages from all neighbours except i are given, i.e.,

$$\bar{\theta}_j^{(l)} \sim \tilde{p}_j(\theta_j) \prod_{i' \in ne(j)/i} m_{i'j}(\theta_j) \text{ for } l = 1, ..., L. \quad (40)$$

These samples are used with kernel approximations in order to represent the message from node j to i (scaled to one), in the NBP approach [26]. We use Gaussian kernels leading to the approximation given by

$$\begin{aligned} \hat{m}_{ji}(\theta_i) &= \sum_{l=1}^{L} \omega_{ji}^{(l)} \mathcal{N}(\theta_i; \theta_{ji}^{(l)}, \Lambda_{ji}), \quad (41) \\ \theta_{ji}^{(l)} &= \tau(\tau^{-1}(\bar{\theta}_j^{(l)}; \theta_j^{(l)}); \theta_i^{(l)}), \\ \omega_{ji}^{(l)} &= \frac{\psi_{i,j}^t(\theta_i^{(l)}, \theta_j^{(l)})}{\sum_{l'=1}^{L} \psi_{i,j}^t(\theta_i^{(l')}, \theta_j^{(l')})}, \end{aligned}$$

where the kernel weights are the normalised edge potentials. Λ_{ji} is related to a *bandwidth* parameter that can be found using Kernel Density Estimation (KDE) techniques. In particular, we use the rule-of-thumb method in [27] and find

$$\begin{aligned} \Lambda_{ji} &= \left(\frac{4}{(2d+1)L} \right)^{2/(d+4)} \hat{\mathbf{C}}_{ji}, \\ \hat{\mathbf{C}}_{ji} &= \sum_{l'} \sum_{l} \omega_{ji}^{(l')} \omega_{ji}^{(l)} (\theta_{ji}^{(l')} - \hat{\mathbf{m}}_{ji})(\theta_{ji}^{(l)} - \hat{\mathbf{m}}_{ji})^T, \\ \hat{\mathbf{m}}_{ji} &= \sum_{l=1}^{L} \omega_{ji}^{(l)} \theta_{ji}^{(l)} \end{aligned}$$

where $\hat{\mathbf{m}}_{ji}$ and $\hat{\mathbf{C}}_{ji}$ are the empirical mean and covariance of the samples, respectively, and d is the dimensionality of θ_{ji}s.

Given these messages, let us consider sampling from the updated marginal in (15). We use the weighted bootstrap (also known as sampling/importance resampling) [28] with samples generated from the (scaled) product of Gaussian densities with mean and covariance found as the empirical mean and covariance of the particle sets, respectively. In other words, given $\hat{\mathbf{m}}_{ji}$ and $\hat{\mathbf{C}}_{ji}$ as above, we generate

$$\begin{aligned} \theta_i^{(l)} &\sim f(\theta_i), \quad l = 1, \cdots, L, \\ f(\theta_i) &\propto \mathcal{N}(\theta_i; \hat{\mathbf{m}}_i, \hat{\mathbf{C}}_i) \prod_{j \in ne(i)} \mathcal{N}(\theta_i; \hat{\mathbf{m}}_{ji}, \hat{\mathbf{C}}_{ji}). \end{aligned}$$

The particle weights for these samples to represent the updated marginal is given by

$$\begin{aligned} \omega_i^{(l)} &= \hat{\omega}_i^{(l)} / \sum_{l'=1}^{L} \hat{\omega}_i^{(l')} \\ \hat{\omega}_i^{(l)} &= \left(p_{0,i}(\theta_i^{(l)}) \prod_{j \in ne(i)} \hat{m}_{ji}(\theta_i^{(l)}) \right) / f(\theta_i^{(l)}) \end{aligned}$$

where $p_{0,i}$ is the prior density selected for θ_i (and, the node potential in (12)). Thus, the local calibration marginal is estimated by

$$\hat{P}_i(\mathrm{d}\theta_i) = \sum_{l=1}^{L} \omega_i^{(l)} \delta_{\theta_i^{(l)}}(\mathrm{d}\theta_i). \quad (42)$$

As the final step of the bootstrap, $\{\theta_i^{(l)}, \omega_i^{(l)}\}_{l=1}^{M}$ is resampled (with replacement) leading to equally weighted particles from $\tilde{p}_i(\theta_i)$, i.e., $\{\theta_i^{(l)}\}_{l=1}^{L}$. We follow similar bootstrap steps in order to generate the samples in (40).

After nodes iterate the BP computations described above for S times, each node estimates its location by finding the empirical mean of $\{\theta_i^{(l)}\}_{l=1}^{L}$. These steps are summarised in Algorithm 1.

Algorithm 1 Pseudo-code for estimation of θ using separable likelihoods within Belief Propagation.

For all $j \in \mathcal{V}$ and $k = 1, \ldots, t$ find $Pois(.; \hat{\lambda}_k^j, \hat{S}_{k,j}(\mathrm{d}x))$ ▷ Local PHD filtering and multi-target estimation
For all $j \in \mathcal{V}$ sample $\theta_i^{(l)} \sim p_{0,i}(\theta_i)$ for $l = 1, \ldots, L$
for $s = 1, ..., S$ **do** ▷ S-steps of LBP
  for all $(i, j) \in \mathcal{E}$ **do** ▷ Evaluate edge potentials
    For all $l = 1, \ldots, L$ and $k = 1, \ldots, t$ find $\hat{p}(Z_k^i | Z_{1:k-1}^j, \theta_{i,j}^{(l)})$
    Find $\psi_{i,j}^k(\theta_i^{(l)}, \theta_j^{(l)})$ in (13) using (20)
  end for
  For all $(i, j) \in \mathcal{E}$ find $\hat{m}_{ji}(\theta_i)$ in (41) ▷ Find LBP messages
  for all $i \in \mathcal{V}$ **do** ▷ Update local marginals
    Find the updated $\hat{P}_i$ in (42) and sample $\theta_i^{(l)} \sim \tilde{p}_i(\theta_i)$
    $\hat{\theta}_i \leftarrow \frac{1}{L} \sum_{l=1}^{L} \theta_i^{(l)}$
  end for
end for

VII. Example

We consider the example scenario depicted in Fig. 2 which consists of a total of 20 manoeuvering objects in a surveillance region. The trajectories are obtained using a linear constant velocity motion model with additive process noise. The MRF model is given by the undirected graph with blue edges. Neighbouring sensors share at least one object in the overlapping part of their FoVs.

The sensors collect range-bearing angle measurements with standard deviations $\sigma_R = 5m$ and $\sigma_\phi = 1^\circ$, respectively. Objects in the FoV are detected with probability one, in this example. The number of false alarms is Poisson distributed with mean $\lambda_{C,i} = 2$ and spatial distribution is uniform in the sensor FoVs. These measurements are filtered locally using the adaptive birth SMC realisation of the PHD filter [25].

Sensor 1 is considered as the origin of the network coordinate system. We use $S = 8$ iterations of a tree-weighted message schedule within the Monte Carlo realisation of the BP steps detailed in Section VI. We provide the estimation error histogram obtained in 100 Monte Carlo simulations in Fig. 3 (for sensors 2–9). The bin width of the histogram is 10m. A very high probability of estimates are in the 2% bound of the minimum distance between any two nodes in the network

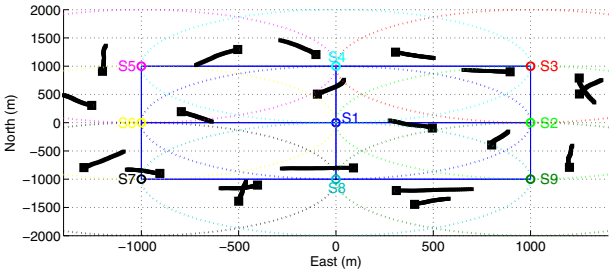

Fig. 2. 9 sensor nodes networked through communication links (blue edges) observing 20 objects. Black curves are the object trajectories with boxes indicating the initial positions. Sensor FoVs are indicated by colored circles.

which is 1000m. The errorneous estimates are due to that the problem has a multi-modal likelihood which can potentially be handled by using better message schedules such as tree-reweighted BP and sophisticated sampling schemes such as stochastic tempering. Development of such sampling strategies remains as future work.

VIII. Conclusion

We proposed a dual-term node-wise separable likelihood for parameter estimation problems in multi-object multi-sensor state space models. This likelihood can be used for cases in which the sensors have partially overlapping FoVs and provide scalability with the number of sensors when used with MRFs, in a problem setting which otherwise has combinatorial complexity.

We exploited message passing algorithms for inference over the proposed graphical model. Doing that, we achieve an efficient computational structure for parameter estimation in state space models. We provided a detailed Monte Carlo algorithm for distributed sensor localisation with complex multi-object measurements. We demonstrate the efficacy our approach in a simulated example.

Acknowledgment

This work was supported by the Engineering and Physical Sciences Research Council (EPSRC) grants EP/J015180/1 and EP/K014277/1, and the MOD University Defence Research Collaboration in Signal Processing.

References

[1] M. P. Dana, *Registration: A prerequisite for multiple sensor tracking*. Artech House, 1990, ch. 5, pp. 155–185.

[2] M. Erol-Kantarci, H. Mouftah, and S. Oktug, "A survey of architectures and localization techniques for underwater acoustic sensor networks," *Communications Surveys Tutorials, IEEE*, vol. 13, no. 3, pp. 487–502, Third Quarter 2011.

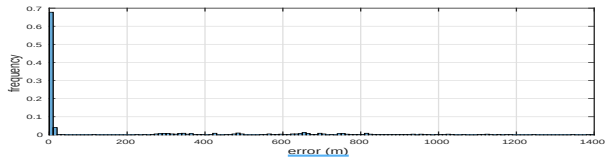

Fig. 3. Histogram of the estimation errors of the proposed algorithm for 100 Monte Carlo runs. The bin-width is 10m.

[3] N. Kantas, A. Doucet, S. S. Singh, J. Maciejowski, and N. Chopin, "On particle methods for parameter estimation in state-space models," *Statist. Sci.*, vol. 30, no. 3, pp. 328–351, 08 2015.

[4] B.-n. Vo, M. Mallick, Y. Bar-shalom, S. Coraluppi, R. Osborne, R. Mahler, B.-t. Vo, and J. G. Webster, *Multitarget Tracking*. John Wiley & Sons, Inc., September 2015.

[5] M. Uney, D. Clark, and S. Julier, "Distributed fusion of PHD filters via exponential mixture densities," *Selected Topics in Signal Processing, IEEE Journal of*, vol. 7, no. 3, pp. 521–531, June 2013.

[6] L. Chen, M. J. Wainwright, M. ÇEtin, and A. S. Willsky, "Data association based on optimization in graphical models with application to sensor networks," *Math. Comput. Model.*, vol. 43, no. 9-10, pp. 1114–1135, May 2006.

[7] M. Cetin, L. Chen, J. Fisher, A. Ihler, R. Moses, M. Wainwright, and A. Willsky, "Distributed fusion in sensor networks: A graphical models perspective," *IEEE Signal Proc. Mag.*, vol. 23, no. 4, pp. 42–55, 2006.

[8] M. Uney and M. Cetin, "Graphical model-based approaches to target tracking in sensor networks: An overview of some recent work and challenges," in *5th ISPA*, 2007, pp. 492–497.

[9] M. Uney, B. Mulgrew, and D. Clark, "A cooperative approach to sensor localisation in distributed fusion networks," *IEEE Trans. on Signal Proc.*, vol. 64, no. 5, pp. 1187–1199, March 2016.

[10] ——, "Latent parameter estimation in fusion networks using separable likelihoods," *IEEE Trans. on Sig. and Info. Proc. Over Net.s*, submitted.

[11] R. P. S. Mahler, *Statistical Multisource Multitarget Information Fusion*. Springer, 2007.

[12] C. Andrieu, A. Doucet, and R. Holenstein, "Particle markov chain monte carlo methods," *Journal of the Royal Statistical Society: Series B (Statistical Methodology)*, vol. 72, no. 3, pp. 269–342, 2010.

[13] J. Ala-Luhtala, N. Whiteley, K. Heine, and R. Piche, "An introduction to twisted particle filters and parameter estimation in non-linear state-space models," *IEEE Trans. on Sig. Proc.*, to appear, 2016.

[14] O. Cappé, S. J. Godsill, and E. Moulines, "An overview of existing methods and recent advances in sequential Monte Carlo," *Proceedings of the IEEE*, vol. 95, pp. 899–924, 2007.

[15] Z. Li, S. Chen, H. Leung, and E. Bosse, "Joint data association, registration, and fusion using em-kf," *Aerospace and Electronic Systems, IEEE Transactions on*, vol. 46, no. 2, pp. 496–507, April 2010.

[16] R. P. S. Mahler, "Multitarget Bayes Filtering via First-Order Multitarget Moments," *IEEE Trans. on Aero. and Elec. Sys.*, vol. 39, no. 4, pp. 1152–1178, Oct. 2003.

[17] A. F. Garcia-Fernandez and B.-N. Vo, "Derivation of the phd and cphd filters based on direct kullback-leibler divergence minimization," *IEEE Trans. on Signal Processing*, vol. 63, no. 21, pp. 5812–5820, Nov 2015.

[18] T. M. Cover and J. A. Thomas, *Elements of Information Theory*. John Wiley & Sons, 1991.

[19] E. Delande, E. Duflos, P. Vanheeghe, and D. Heurguier, "Multi-sensor phd: Construction and implementation by space partitioning," in *IEEE ICASSP 2011*, May 2011, pp. 3632–3635.

[20] M. J. Wainwright and M. I. Jordan, "Graphical models, exponential families, and variational inference," *Found. Trends Mach. Learn.*, vol. 1, no. 1-2, pp. 1–305, Jan. 2008.

[21] J. S. Yedidia, W. T. Freeman, and Y. Weiss, "Understanding belief propagation and its generalizations," MERL Tech. Rep., Jan. 2002.

[22] M. Uney, B. Mulgrew, and D. Clark, "Target aided online sensor localisation in bearing only clusters," in *SSPD*, Sept 2014, pp. 1–5.

[23] J. Kingman, *Poisson Processes*, ser. Oxford Studies in Probability. Clarendon Press, 1992.

[24] G. Casella and C. P. Robert, *Monte Carlo Statistical Methods*, 2nd ed. Springer, 2005.

[25] B. Ristic, D. Clark, B.-N. Vo, and B.-T. Vo, "Adaptive target birth intensity for PHD and CPHD filters," *Aerospace and Electronic Systems, IEEE Transactions on*, vol. 48, no. 2, pp. 1656–1668, 2012.

[26] E. B. Sudderth, A. T. Ihler, M. Isard, W. T. Freeman, and A. S. Willsky, "Nonparametric belief propagation," *Commun. ACM*, vol. 53, no. 10, pp. 95–103, Oct. 2010.

[27] B. Silverman, *Density Estimation for Statistics and Data Analysis*. Chapman and Hall, 1986.

[28] A. F. M. Smith and A. E. Gelfand, "Bayes statistics without tears: A sampling-resampling perspective," *The American Statistician*, vol. 46, no. 2, pp. 84–88, May 1992.